

Ab Initio and Kinetic Study on CH₃ Radical Reaction with H₂CO

Cheng-bin Che, Hui Zhang, Xiang Zhang, Yue Liu,* and Bo Liu

School of Chemical and Environmental Engineering, Harbin University of Science and Technology, Harbin, 150080, P. R. China

Received: November 10, 2002; In Final Form: February 25, 2003

Ab initio calculations on the reaction of the CH₃ radical with H₂CO were carried out at the CCSD(T)/6-311G(2df,p)//B3LYP/6-311+G(d,p) level. Three possible reaction pathways, the H-abstraction pathway RI, the C-addition pathway RII, and the O-addition pathway RIII, were considered. The entrance barrier heights of the three pathways at the CCSD(T) level are 40.20, 34.02, and 69.45 kJ mol⁻¹, respectively. Although the C-addition pathway has the lowest entrance barrier height, calculated rate constants using canonical variational transition state theory incorporating with small-curvature tunneling correction (CVT/SCT) show that the H-abstraction pathway is the fastest reaction channel in a wide temperature region of 300–2000 K. The C-addition pathway has considerable contribution only at the low-temperature region. The O-addition pathway is too slow and can be ruled out over the whole temperature region.

Introduction

CH₃ radical reaction with H₂CO is of importance in many high-temperature processes of organic compounds, typically, in the decomposition and oxidation of ethers such as CH₃OCH₃ and *t*-C₄H₉OCH₃ and the oxidation and pyrolysis of methanol. This reaction is also of great interest in atmospheric chemistry.¹ To know the details of the mechanism and kinetics of this reaction, many experiments have been carried out to analyze the products and to measure the rate constants and temperature dependence over wide temperature region. Based on the analysis of final products, the main reaction channel was suggested to be the direct H-abstraction process.^{2–11} The earliest experiment of Kodama and Takezaki gave a lower activation energy of 23.43 kJ mol⁻¹ for this reaction.² In 1959, Kutschke and co-workers^{3,4} reported two kinetic studies of this reaction with the methyl radical produced by photolysis of azomethane or pyrolysis of di-butyl peroxide in the presence of formaldehyde. They suggested an activation energy of 26.8 kJ mol⁻¹ and a preexponential factor of 2.5×10^{-13} cm³ molecule⁻¹ s⁻¹ for this reaction in the temperature range from 353 to 453 K. Manthorne and co-workers^{5,6} studied the methyl radical reactions in the pyrolysis of dimethyl ether. In one paper,⁵ they reported the activation energy of 45 kJ mol⁻¹ and the preexponential factor of 2.1×10^{-11} cm³ molecule⁻¹ s⁻¹ based on the results at 788, 856, and 935 K. These values are greater than the low-temperature results of Kutschke et al.^{3,4} In another experiment at 1005 K,⁶ they obtained a rate constant of 5.25×10^{-14} cm³ molecule⁻¹ s⁻¹ which is lower by a factor 2 than the extrapolated value from their former Arrhenius parameters. In Aronowitz et al.'s kinetic experiment of pyrolysis of dimethyl ether in the temperature range from 790 to 950 K,⁷ they estimated that the rate constant of this reaction was between 1.3×10^{-12} and 7.5×10^{-12} cm³ molecule⁻¹ s⁻¹. It should be noted that, all of these early kinetic studies are indirect ones and exist significant differences. In 1983, Anastasi⁸ reported the first direct measurement on the reaction of methyl with formaldehyde by molecular

modulation spectrometer (MMS) and studied the products with gas chromatography and performed kinetic analysis. In the temperature range from 500 to 603 K, they suggested an Arrhenius expression of $(1.4 \pm 0.1) \times 10^{-12} \exp(-29.1 \pm 0.4 \text{ kJ mol}^{-1}/RT)$. In this paper, Anastasi mentioned Selby's results⁹ in a smaller temperature range (399–434 K). Selby⁹ gave a higher value for both *E* (32.3 kJ mol⁻¹) and *A* (1.66×10^{-12} cm³ molecule⁻¹ s⁻¹). Choudhury and Lin investigated the high-temperature rate constant for this reaction in the temperature range from 1170 to 1630 K with shock tube technology¹⁰ and kinetic modeling.^{10,11} An Arrhenius expression of $1.7 \times 10^{-9} \pm 0.4 \exp(-11600 \pm 1260/T)$ cm³ molecule⁻¹ s⁻¹ confirms the earlier observations that, at temperatures above 1000 K, the Arrhenius plot curves upward. Their standard TST calculation with Eckart tunneling correction predicted a significant tunneling effect at low temperature, whereas the tunneling effect was small at high temperature. However, it is obvious that the parameters used in their TST calculations were artificially adjusted for fitting the experimental results.

It is obvious that the measured kinetic parameters for the title reaction have great discrepancy between different experiments. Moreover, the contributions of other possible pathways, such as the C-addition and the O-addition pathways, have not been carefully considered, and their contributions have not been evaluated. For the C-addition pathway, several gas-phase experiments^{12–14} indicated a barrier of 28.5 kJ mol⁻¹, and the theoretical calculations gave the barrier of 26.4 and 27 kJ mol⁻¹ at the PMP4/6-31G(d)¹⁵ and the G2 levels,¹⁶ respectively. One can easily notice that these predicted barrier heights for the C-addition channel are close to those of the H-abstraction channel, but till now, no compelling explanation on why the C-addition channel is of less important in CH₃ + H₂CO reaction is given, and detailed kinetic analysis is needed.

This paper presents a theoretical study on mechanism and kinetics of the title reaction based on high-level ab initio calculations and canonical variational transition state theory incorporating with small curvature tunneling correction (CVT/SCT) on various possible reaction pathways. The predominant

* To whom correspondence should be addressed. Department of Chemistry, Harbin Normal University, 150080 China. E-mail: yuesd@0451.com.

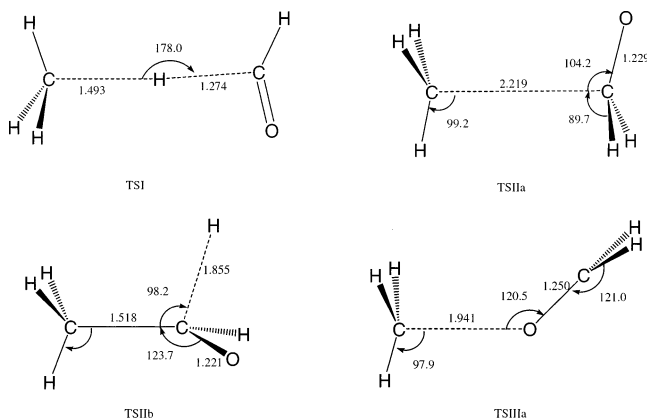


Figure 1. Optimized transition state structures at the B3LYP/6-311+G(d,p) level.

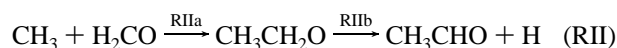
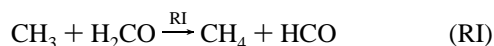
mechanism for the title reaction is confirmed to be the H-abstraction pathway.

Computational Method

Geometries of reactants and products and transition states were fully optimized at the B3LYP/6-311+G(d,p) level using the Gaussian 98 program.¹⁷ Reaction paths from transition state structures to both reactants and products sides were carried out with step-size 5 (amu)^{1/2} bohr using the intrinsic reaction coordinate (IRC) method to ensure that the transition states are really located on the corresponding pathways. To obtain more reliable energies, CCSD(T)/6-311G(2df,p) single-point energy calculations were performed at the stable structures optimized by the B3LYP method. The Polyrate 8.0 program provided by Truhlar¹⁸ was used to calculate the rate constants and temperature dependences. Traditional transition state theory (TST), canonical variational transition state theory (CVT), and canonical variational transition state theory incorporating with small curvature tunneling correction (CVT/SCT) were used in rate constants calculations. In rate constants calculations, all of the vibration modes were treated harmonically.

Results and Discussions

Three reaction pathways for different reactive sites in formaldehyde attacked by the methyl radical are as follows: (1) The direct H-abstraction pathway, which leads to CH₄ and HCO (RI). It is an elementary process through a near-linear transition state TSI. (2) The C-addition pathway (RII), which initially forms an intermediate adduct CH₃CH₂O (step RIIa) then eliminates an H atom to form CH₃CHO molecule (step RIIb). Two transition states, TSIIa and TSIIb, are located respectively in RIIa and RIIb. (3) The O-addition pathway (RIII), first a CH₃ radical adds to the O atom of H₂CO molecule forming an intermediate CH₃OCH₂ (step RIIIa) and then the CH₃OCH₂ radical dissociates to a CH₃O radical and a CH₂ radical (step RIIIb). A transition state TSIIIa was found for RIIIa, but no transition state was found for RIIIb



The optimized transition state structures are shown in Figure 1, where relevant geometric parameters have been indicated.

In Figure 2, the reaction profiles are shown with the relative energies at both the B3LYP and CCSD(T) levels. The calculated electronic energies, zero-point energies, and total energies for all of the stable species involved in the reaction of CH₃ + H₂CO at both the B3LYP and CCSD(T) levels, and the relative energies of products, intermediates, and transition states at the B3LYP/6-311+G(d,p) and the CCSD(T)/6-311G(2df,p)//B3LYP/6-311+G(d,p) levels (set the sum of the total energies of reactants to zero) are given in Table 1. The calculated harmonic frequencies for all of the stable species involved in the reaction of CH₃ + H₂CO at the B3LYP level are given as Supporting Information.

Among the three pathways, the H-abstraction pathway RI is the one with the largest exothermal heat. The reaction heats of RI calculated by the B3LYP and the CCSD(T) methods, -67.25 and -71.36 kJ mol⁻¹, are in good agreement with the results -71 kJ mol⁻¹ at the B3LYP/6-311+G(2df,p)//B3LYP/6-31G(d) level and -69 kJ mol⁻¹ at the G2 level of theory in Boyd et al.'s work¹⁶ but respectively greater by 6.10 and 10.21 kJ mol⁻¹ in value than -61.15 kJ mol⁻¹ based on the heats of formation of CH₃, H₂CO, CH₄, and HCO.¹⁹ From thermochemistry, the H-abstraction pathway RI should be the most predominant pathway for the CH₃ radical reacted with H₂CO. For the C-addition and the O-addition pathways, the intermediates, CH₃-CH₂O and CH₃OCH₂, produced by the initial steps RIIa and RIIIa are more stable than the initial reactants by 38.07 and 23.30 kJ mol⁻¹ at the CCSD(T) level, respectively, and also more stable than the final products by 49.83 and 391.56 kJ mol⁻¹ respectively. So the intermediates CH₃CH₂O and CH₃OCH₂ are respectively the most stable species along RII and RIII.

For RIII, both the B3LYP and CCSD(T) methods gave a much higher barrier for its initial step RIIIa compared with those for the H-abstraction pathway RI and the initial step of the C-addition pathway RIIa, and step RIIIb needs a very high dissociation energy. So, the O-addition pathway is expected to be the slowest one and can be excluded from the CH₃ reaction with H₂CO. At the B3LYP level, the calculated barrier height of 23.32 kJ mol⁻¹ for RI is slightly lower than the barrier height of 25.05 kJ mol⁻¹ for RIIa, but at the CCSD(T) level, the barrier height of 40.20 kJ mol⁻¹ for RI is even higher than the barrier height of 34.00 kJ mol⁻¹ for RIIa. Because TSIIb is located 11.63 and 25.61 kJ mol⁻¹ higher than TSIIa respectively at the CCSD(T) and B3LYP levels, the dissociation of CH₃CH₂O to CH₃CHO + H should be slower than to the reactants CH₃ + H₂CO. It is also easy to know that the reaction equilibrium does not favor the H-elimination products CH₃CHO + H because they are higher in energy than the initial reactants as well as the intermediate CH₃CH₂O, so we can assert that RIIb is not important in the total reaction mechanism. Therefore, to know whether the H-abstraction pathway or the C-addition pathway is the most predominant one in the CH₃ + H₂CO reaction, what we should do is to know whether RI or RIIa is the faster one.

Boyd et al.¹⁶ also reported relatively higher activation enthalpy for the H-abstraction pathway than that for the C-addition pathway at both the B3LYP/6-311+G(2df,p)//B3LYP/6-31G(d) and G2 levels. Here we would like to note that the relative energy difference between our work (Table 1 and Figure 2) and Boyd et al.'s work is caused not only by the different theoretical levels but also by the different calculation method. Different to Boyd et al.'s work,¹⁶ the zero-point energies were not corrected by a scale factor and the thermal and enthalpy corrections (298 K) were not considered in relative energy calculations in this work. We have checked that the relative enthalpies (298 K) at

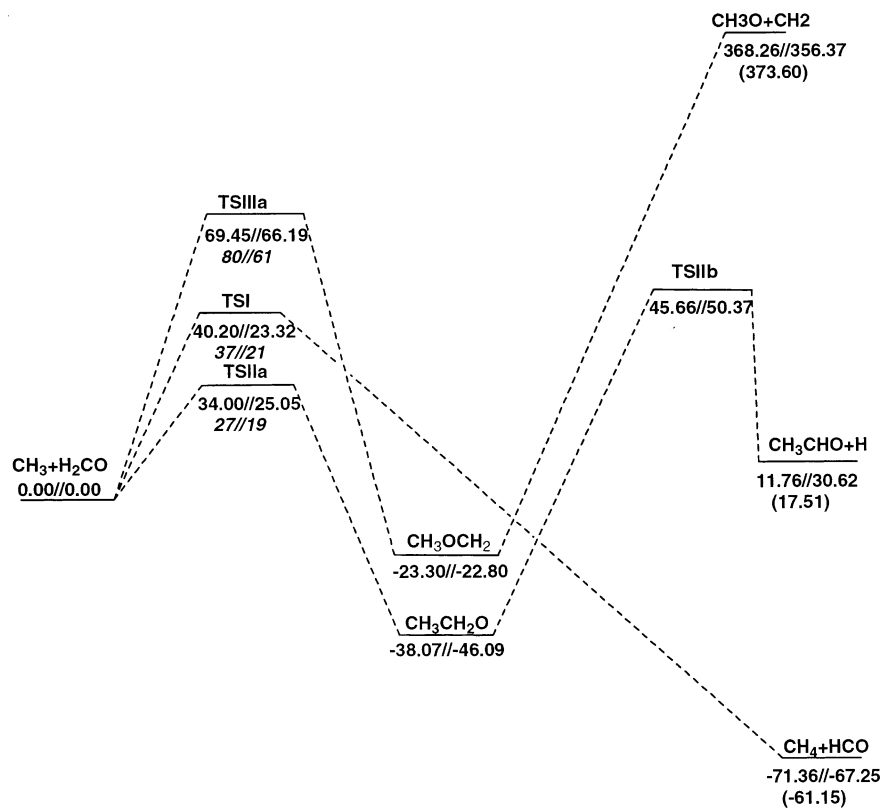


Figure 2. Energy profiles of reaction pathways of methyl with formaldehyde. Relative energies (in kJ mol⁻¹) of stationary structures are given by CCSD(T)//B3LYP, and the values in parentheses are calculated based on the available heats of formation on NIST Chemistry WebBook.¹⁹

TABLE 1: Electronic Energies (E_e), Zero-Point Energies (E_{zpe}), Total Energy (E_t), and Relative Energy (E_r) of the Stable Structures

species	E_e (hartrees) ^a	E_{zpe} (kJ mol ⁻¹)	E_t (hartrees) ^a	E_r (kJ mol ⁻¹) ^a	ΔH_{298} (kJ mol ⁻¹) ^b		
					B3	G2	exp.
CH ₃	-39.7501042// -39.8551666	77.82	-154.0127182// -154.3407798	0.00//0.00		0.00	0.0
H ₂ CO	-114.3187566// -114.5417558	69.58					
CH ₄	-40.4251543// -40.5339328	116.94	-154.0398991// -154.3663957	-71.36// -67.25	-71	-69	-61.15
HCO	-113.6722579// -113.8912668	34.06					
CH ₃ CH ₂ O	-154.0915045// -154.4226127	168.78	-154.0272186// -154.358333	-38.07// -46.09	-54	-40	
CH ₃ OCH ₂	-154.0869776// -154.4148437	171.67	-154.021592// -154.349464	-23.30// -22.80	-31	-32	
CH ₂ ³ A	-39.0696841// -39.1660808	45.02	-153.872454// -154.205043	368.26//356.37			373.58
CH ₃ O	-114.8560122// -115.0922131	94.77					
CH ₃ CHO	-153.5636165// -153.882148	144.89	-154.0082406// -154.3291175	11.76//30.62			17.51
H Atom	-0.4998098// -0.5021559	0.00					
TSI	-154.0522735// -154.3867646	144.06	-153.9974058// -154.3318969	40.20//23.32	21	37	
TSIIa	-154.0605315// -154.3920017	159.54	-153.9997675// -154.3312377	34.00//25.05	19	27	
TSIIb	-154.0521705// -154.3783257	149.24	-153.9953267// -154.3215935	45.66//50.37			
TSIIIa	-154.0463459// -154.3756493	157.74	-153.9862671// -154.315570	69.45//66.19	61	80	

^a Energies are given as $E_{CCSD(T)}/E_{B3LYP}$. ^b Relative enthalpies at 298 K calculated at the B3LYP/6-311+G(2df,p)//B3LYP/6-31G(d) and G2 levels in ref 16. ^c Heat of formation from NIST Chemistry WebBook (in kJ mol⁻¹).¹⁹ CH₃ radical, 145.69; H₂CO, -115.90; CH₄, -74.87; HCO, 43.51; CH₃O, 17 ± 4; CH₂, 386.39; CH₃CHO, -170.7 ± 1.5; H, 218.00.

the B3LYP/6-311+G(2df,p)//B3LYP/6-311+G(d,p) level are nearly the same with the relative energies at the B3LYP/6-311+G(2df,p)//B3LYP/6-31G(d) level using the same calculation method in Boyd et al.'s work.¹⁶ For example, the activation enthalpies of RI and RIIa calculated using the same method but at the B3LYP/6-311+G(2df,p)//B3LYP/6-311+G(d,p) level are respectively 20.69 and 18.79 kJ mol⁻¹ (298 K), whereas Boyd et al.'s result are respectively 21 and 19 kJ mol⁻¹ at the B3LYP/6-311+G(2df,p)//B3LYP/6-31G(d) level.

In the reaction of H₂CO with other radicals, the H-abstraction barrier is usually much lower than the addition barrier, so it is easy to know that the H-abstraction pathway is the dominant one. For example, the barrier of an OH radical adding to H₂CO is 33.5 kJ mol⁻¹ higher than that of the OH radical abstracting

a H atom from H₂CO at the CCSD(T) level.²⁰ However, it is difficult to determine which is the more favorite one in the H₂CO + CH₃ reaction on the base of barriers of the two channels, because their barrier difference is small at the B3LYP levels, whereas CCSD(T) single-point energy calculations gave a relative higher barrier for the H-abstraction. To determine the dominant reaction channel theoretically, rate constants calculations are desirable.

To evaluate the contribution of each pathway to the lose rate of the reactants, the theoretical rate constants for the entrance steps of the three pathways are discussed and compared with experimental results in the following section. It should be noted that, for considering variational effects and small tunneling corrections using the barrier heights at the CCSD(T)//B3LYP

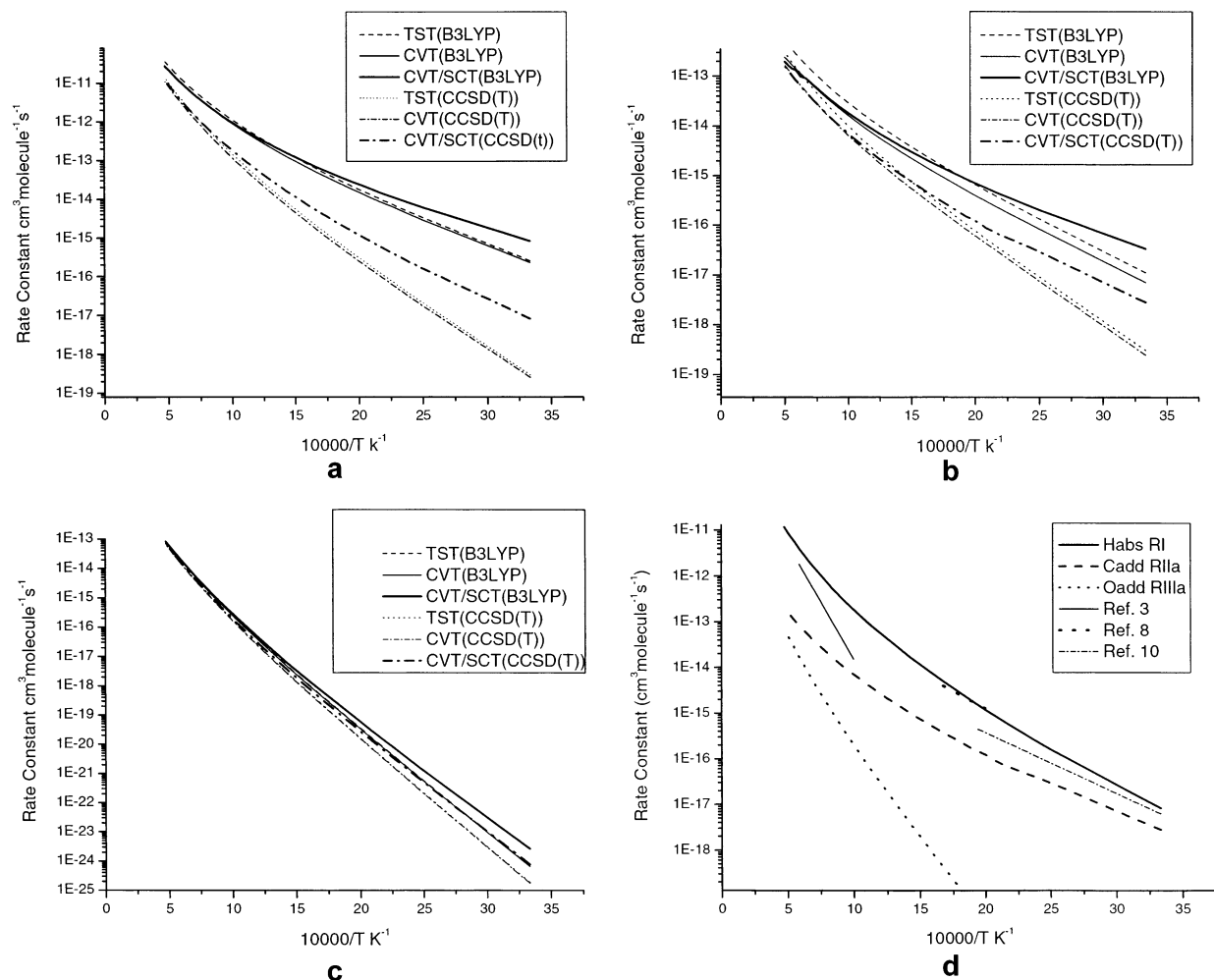


Figure 3. (a) Calculated rate constants of the H-abstraction pathway RI of the methyl radical reaction with formaldehyde. (b) Calculated rate constants for the C-addition pathway step RIIa of the methyl radical reaction with formaldehyde. (c) Calculated rate constants for the O-addition pathway step RIIIa of the methyl radical reaction with formaldehyde. (d) Comparison of calculated CVT/SCT rate constants for the H-abstraction pathway RI, the C-addition step RIIa, and the O-addition step RIIIa, and two direct experimental results of methyl radical reaction with formaldehyde

level, the minimum energy reaction paths (MEPs) at the B3LYP/6-311+G(d,p) level were scaled by the ratio of the classical barrier height at the CCSD(T) level to that at the B3LYP level, $V_{\text{MEP}}[\text{TS}(\text{CCSD}(\text{T}))]/V_{\text{MEP}}[\text{TS}(\text{B3LYP})]$. In Figure 3a–c, the calculated TST, CVT, and CVT/SCT rate constants are plotted against the reciprocal of temperature between 300 and 2000 K for RI, RIIa, and RIIIa, respectively. In Figure 3d, their CVT/SCT rate constants at the CCSD(T) and the experimental results are compared.

From Figure 3a–c, it is easy to see that, because of the lower barrier heights, the calculated rate constants for the H-abstraction pathway RI, the C-addition step RIIa, and the O-addition step RIIIa using the barrier heights calculated at the B3LYP level are greater than the corresponding results using the barrier heights calculated at the CCSD(T) level. For the three pathways, the variational effect is of less importance in rate constant calculations in the whole temperature region; small curvature tunneling correction plays less important role at high temperature but should be considered at the low-temperature region.

Figure 3d shows the comparison of the CVT/SCT rate constants of the three pathways calculated at the CCSD(T) level with the experimental results. Because of the higher barrier, the CVT/SCT rate constants of RIIIa are much smaller than all of the experimental rate constants of the $\text{CH}_3 + \text{H}_2\text{CO}$ reaction, so the contribution of the O-addition pathway to the reaction of $\text{CH}_3 + \text{H}_2\text{CO}$ can be ruled out. Although the barrier height

of RI is higher than that of RIIa at the CCSD(T) level, its CVT/SCT rate constants are greater than those of RIIa over the whole temperature region. For example, at 300 and 2000 K, the calculated CVT/SCT rate constants of RI, are respectively about 3 and 60 times as much as that of RIIa. Given in the Supporting Information, the calculated low real frequencies of TSI are smaller than those of TSIIa, especially for the lowest frequency (20 cm⁻¹ for TSI and 131 cm⁻¹ for TSIIa) at the B3LYP/6-311+G(d,p) level. From a theoretical point of view, lower values of these frequencies will cause a greater vibration partition function for TSI than that of TSIIa and, thus, a much greater preexponential factor *A* for RI than that of RIIa. So it is not surprising that RI is faster than RIIa although the barrier height of RI is slight higher than that of RIIa.

Compared with previous kinetic experimental results, our calculated rate constants at the CCSD(T) level for the H-abstraction reaction RI are consistent with Kutschke and co-workers' results³ (300–500 K) and Anastasi's results⁸ (500–603 K) at the low-temperature region and somewhat greater than the results of Choudhury and Lin et al.¹⁰ at the high-temperature region (1170–1630 K), but the maximum difference is less than 9 times. A greater account of the comparison between our theoretical rate constants with other indirect experimental results is not given here. Although the potential energy surface at current theoretical levels may not be accurate enough for predicting accurate values of rate constants for the

CH₃ reaction with H₂CO, this theoretical investigation clarifies that the H-abstraction is predominant at both low and high temperature, whereas the C-addition reaction may have considerable contributions at low temperatures. The O-addition reaction pathway's contribution can be ignored at both low and high-temperature regions.

Conclusion:

Ab initio and canonical variational transition state theory calculations were performed to study the mechanism and kinetics of the CH₃ + H₂CO reaction. At the CCSD(T)/6-311G(2df,p)//B3LYP/6-311+G(d,p) level, the predicted barrier height for the H-abstraction pathway RI is higher than that for the C-addition pathway RIIa, but the calculated CVT/SCT rate constants for the H-abstraction pathway RI are greater than those for the initial step RIIa of the C-addition pathway over the temperature range 300–2000 K. The theoretical CVT/SCT rate constants for the H-abstraction pathway RI are in good agreement with two previous low-temperature experimental results (300–603 K)^{3,8} and somewhat greater than the high-temperature results (1170–1630 K).¹⁰ At the low-temperature region, the contribution of the C-addition pathway becomes important and should be considered. The O-addition pathway is too slow over the whole temperature range and can be ignored from the CH₃ + H₂CO reaction mechanism.

Supporting Information Available: The calculated harmonic frequencies for all the stable species involved in the reaction of CH₃ + H₂CO at the B3LYP level. This material is available free of charge via the Internet at <http://pubs.acs.org>.

References and Notes

(1) (a) Westbrook, C. K.; Dryer, F. L. *Combustion Sci. Technol.* **1979**, *20*, 125. (b) Aronowitz, D.; Naegli, D. W.; Glassman, I. *J. Phys. Chem.* **1977**, *81*, 2555. (c) Allara, D. L.; Mill, T.; Hendry, G. D.; Mayo, F. R. *Adv. Chem. Ser.* **1968**, No. 76. 40. (d) Demerjian, K. L.; Krerr, J. A.;

Calvert, J. G. *Adv. Environ. Sci. Technol.* **1974**, *4*, 1. (e) Adamic, K.; Howard, J. A.; Ingold, K. U. *Can. J. Chem.* **1969**, *47*, 3803. (f) Benson, S. W. *Thermochemical Kinetics*, 2nd, ed.; Wiley: New York, 1976; p 239. (g) Pate, C. T.; Finlayson, B. J.; Pitts, J. N., Jr. *J. Am. Chem. Soc.* **1974**, *96*, 6554.

- (2) Kodama, S.; Takezaki, Y. *J. Chem. Soc. Jpn.* **1952**, 73, 13.
 (3) Toby, S.; Kutschke, K. O. *Can. J. Chem.* **1959**, *37*, 672.
 (4) Blake, A. R.; Kutschke, K. O. *Can. J. Chem.* **1959**, *37*, 1462.
 (5) Held, A. M.; Manthorne, K. C.; Pacey, P. D.; Reinholdt, H. P. *Can. J. Chem.* **1977**, *55*, 4128.
 (6) Manthorne, K. C.; Pacey, P. D. *Can. J. Chem.* **1978**, *56*, 1307.
 (7) Aronowitz, D.; Naegli, D. *Int. J. Chem. Kinet.* **1977**, *9*, 471.
 (8) Anastasi, C. *J. Chem. Soc., Faraday Trans. 1* **1983**, *79*, 749.
 (9) Selby, K. R. Ph.D. Thesis, University of York, 1978.
 (10) Choudhury, T. K.; Sanders, W. A.; Lin, M. C. *J. Phys. Chem.* **1989**, *93*, 5143–5147.
 (11) Choudhury, T. K.; Sanders, W. A.; Lin, M. C. *J. Chem. Soc., Faraday Trans. 2* **1989**, *85* (7), 801–808.
 (12) Batt, L.; Milne, R. T. *Int. J. Chem. Kinet.* **1977**, *9*, 549.
 (13) Batt, L. *Int. J. Chem. Kinet.* **1979**, *11*, 977.
 (14) Choo, K. Y.; Benson, S. W. *Int. J. Chem. Kinet.* **1981**, *13*, 833.
 (15) Gonzalez, C.; Sosa, C.; Schlegel, H. B. *J. Phys. Chem.* **1989**, *93*, 2435–2440.
 (16) Boyd, S. L.; Boyd, R. J. *J. Phys. Chem. A* **2001**, *105*, 7096–7105.
 (17) Frisch, M. J.; Trucks, G. W.; Schlegel, H. B.; Scuseria, G. E.; Robb, M. A.; Cheeseman, J. R.; Zakrzewski, V. G.; Montgomery, J. A., Jr.; Stratmann, R. E.; Burant, J. C.; Dapprich, S.; Millam, J. M.; Daniels, A. D.; Kudin, K. N.; Strain, M. C.; Farkas, O.; Tomasi, J.; Barone, V.; Cossi, M.; Cammi, R.; Mennucci, B.; Pomelli, C.; Adamo, C.; Clifford, S.; Ochterski, J.; Petersson, G. A.; Ayala, P. Y.; Cui, Q.; Morokuma, K.; Malick, D. K.; Rabuck, A. D.; Raghavachari, K.; Foresman, J. B.; Cioslowski, J.; Ortiz, J. V.; Stefanov, B. B.; Liu, G.; Liashenko, A.; Piskorz, P.; Komaromi, I.; Gomperts, R.; Martin, R. L.; Fox, D. J.; Keith, T.; Al-Laham, M. A.; Peng, C. Y.; Nanayakkara, A.; Gonzalez, C.; Challacombe, M.; Gill, P. M. W.; Johnson, B. G.; Chen, W.; Wong, M. W.; Andres, J. L.; Head-Gordon, M.; Replogle, E. S.; Pople, J. A. *Gaussian 98*; Gaussian, Inc.: Pittsburgh, PA, 1998.
 (18) Chuang, Y.-Y.; Corchado, J. C.; Fast, P. L.; Villà, J.; Hu, W.-P.; Liu, Y.-P.; Lynch, G. C.; Nguyen, K. A.; Jackels, C. F.; Gu, M.-Z. Rossi, I.; Coitiño, E. L.; Clayton, S.; Melissas, V. S. *POLYRATE*, version 8.0; University of Minnesota: Minneapolis, MN, 1998.
 (19) Frequencies and heats of formation of some species are taken from NIST Chemistry WebBook.
 (20) Alvarez-Idaboy, J. R.; Mora-Diez, N.; Boyd, R. J.; Vivier-Bunge, A. *J. Am. Chem. Soc.* **2001**, *123*, 2018–2024.